

Characterization of Limestone as Raw Material to Hydrated Lime

Rajeb Salem Hwidi¹, Tengku Nuraiti Tengku Izhar^{1,*}, and Farah Naemah Mohd Saad¹

¹School of Environmental Engineering, Universiti Malaysia Perlis, Kompleks Pusat Pengajian Jejawi 3, Arau 02600, Perlis, Malaysia.

Abstract. In Malaysia, limestone is essentially important for the economic growth as raw materials in the industry sector. Nevertheless, a little attention was paid to the physical, chemical, mineralogical, and morphological properties of the limestone using X-ray fluorescence (X-RF), X-ray diffraction (X-RD), Fourier transform infrared spectroscopy (FTIR), and Scanning electron microscopy / energy dispersive x-ray spectroscopy (SEM-EDS) respectively. Raw materials (limestone rocks) were collected from Bukit Keteri area, Chuping, Kangar, Perlis, Malaysia. Lab crusher and lab sieved were utilized to prepare five different size of ground limestone at (75 μm , 150 μm , 225 μm , 300, and 425 μm) respectively. It is found that the main chemical composition of bulk limestone was Calcium oxide (CaO) at 97.58 wt.% and trace amount of MnO, Al₂O₃, and Fe₂O₃ at 0.02%, 0.35%, and 0.396% respectively. XRD diffractograms showed characteristic peaks of calcite and quartz. Furthermore, main FTIR absorption bands at 1,419, 874.08 and 712.20 cm^{-1} indicated the presence of calcite. The micrographs showed clearly the difference of samples particle size. Furthermore, EDS peaks of Ca, O, and C elements confirmed the presence of CaCO₃ in the samples.

1 Introduction

In Malaysia, limestone is characterized by wide karstification with the development of a complex and large network of caves [1]. Limestone hills naturally with sharp sides and rising up to many hundred meters above the flat alluvial plains are a well-known feature of the Malaysian landscape. Most of these alluvial plains are underlain at moderately shallow depths by the same limestone that forms, the prominent hills. The detection of rich tin deposits in the alluvium has led to the improvement of several urban centers adjacent to and later increasing on to the former mining regions [1].

Limestone is mainly composed of calcium carbonate mineral CaCO₃. This compound is one of the most common materials among the chemically precipitated sedimentary rocks [2]. Biological and also biochemical methods are the main processes in the carbonate sediments formation. Nevertheless, the inorganic precipitation of calcium carbonate from seawater can also happen [3]. After CaCO₃ formation, physical and chemical processes of diagenesis can significantly change the characteristics of CaCO₃.

* Corresponding author: nuraiti@unimap.edu.my

Limestone is widely used in architectural applications for walls, decorative trim and veneer. It is less frequently used as a sculptural material, because of its porosity and softness. However, it is a common base material. It may be found in both bearing (structural) and veneer applications. In Malaysia, limestone is recently used in removal of heavy metals (Pb, Cd, Cu, Ni, Zn, and Cr(III)) from water [4]. It's found that limestone was able to remove more than 90% of heavy metals from polluted water [4].

Another important use of limestone (after converting to hydrated lime) is mitigation of poisonous and dangerous gases emission. Lime treatment reduces odors, particularly hydrogen sulfide, which is not only a nuance odor but also can be very dangerous if localized high concentrations build up [5]. In addition to high pH, lime provides free calcium ions, which react and form complexes with odorous sulfur species such as hydrogen sulfide and organic mercaptans [5, 6].

In the current work, the characterization of limestone as a raw material of hydrated lime was conducted using wide range of analysis to investigate the physical, chemical, mineralogical, and morphological properties of limestone.

2 Materials and methods

2.1 Sample location

The main material used in this work is the limestone, which was obtained from Bukit Keteri area, Chuping, 02450 Kangar, Perlis, Malaysia, 6.5035795,100.26139 GPS coordination.

2.2 Sample preparation

In order to prepare the samples, limestone were crashed using lab crusher. The ground limestone samples were sieved into five different sizes at 75 μm , 150 μm , 225 μm , 300, and 425 μm as shown in Figure 1.



Fig. 1. Optical images of limestone samples at (a) 75 μm , (b) 150 μm , (c) 250 μm , (d) 300, and (e) 425 μm .

2.3 Sample characterization

After preparation of limestone samples, the mineralogical, chemical, physical and morphological properties of the hydrated lime samples were characterized and evaluated using X-ray fluorescence (X-RF) spectrometry, X-ray diffraction (X-RD), Fourier Transform Infrared Spectroscopy (FTIR), and Scanning Electronic Microscopy (SEM) attached with Energy Dispersive X-ray analysis (EDS) respectively.

2.3.1 X-ray fluorescence (X-RF)

X-rays fluorescent (XRF) was conducted using XRF spectrometer (Model MiniPAL 4 Brand: PANalytical PW4030). X-RF analysis was carried out to determine elemental composition of the materials, which is based on the principle of individual atoms. When the sample is irradiated by X-rays, it measures the individual component wavelengths of the fluorescent emission produced by the sample.

2.3.2 X-ray diffraction (X-RD)

First, the specimen was pressed in stainless steel holder and then the Quantitative mineralogical evaluation was conducted by X-ray diffraction (X-RD) using CuK α radiation, 0.02° step size, 3 s counting time, 10° b 2 θ b 80° range and Rietveld refinement method (X'Pert MPD - PANalytical X-ray B.V.). This method is designed to obtain a high quality diffraction data, associated with ease of use and flexibility to quickly switch to different applications.

2.3.3 Fourier transform infrared spectroscopy (FTIR)

Transmission FTIR spectra of composite films were recorded from thin KBr disc of the samples with Perkin Elmer 2000 FTIR spectrophotometer at room temperature. The samples were scanned from 4000 to 400 cm⁻¹ with resolution of 0.4 cm⁻¹. By using FTIR, the functional groups in a molecule can be identified.

2.3.4 Scanning electron microscopy / energy dispersive x-ray spectroscopy (SEM-EDS)

The morphology and elemental chemical composition of the limes were determined respectively by scanning electronic microscopy (SEM) – using secondary electrons detector – and energy dispersive X-ray analysis (EDS) (LEO Stereoscan 440). The specimens were coated by an extremely thin layer of gold (1.5 - 3 nm) using sputter coater machine. The purpose of specimens coating is to avoid the poor resolution of the image and also to prevent the electrostatic charging during test. The test was conducted at 1000x magnification.

3 Results and discussions

The chemical composition of bulk limestone is listed in Table 1. The high contents of Calcium oxide (CaO) (97.58 wt.%) in the sample indicated that the sample was high limestone purity [7], but silica constituted the common impurity (0.90 wt.%). The high percentage of the main element (CaO) in the specimen showed high enrichment factor thus concerning cement as the main contributing source to airborne particulate matter in these

factories and environs. This has a clear environmental implication, which should be of interest to the environmental protection agency and also to the government. The occurrence of faint magnesium oxide in the sample bears witness to the presence of trace amounts of smectite [7, 8]. It is also found that a trace amount of Al_2O_3 , Fe_2O_3 , and SrO elements are existed in the sample.

Table 1. Chemical composition of bulk limestone sample (wt.%).

Chemical Compound	Al Al ₂ O ₃	Si SiO ₂	Ca CaO	Ti TiO ₂	Mn MnO	Mg MgO	Fe Fe ₂ O ₃	Cu CuO	Sr SrO	Ru RuO ₂	Eu Eu ₂ O ₃	Total
Weight %	0.35	0.90	97.58	0.13	0.02	0.01	0.395	0.065	0.092	0.37	0.08	100

Fig. 2 shows the XRD diffractograms of the representative limestone samples, indicating the presence of characteristic peaks of calcite as identified by the distinctive reflections at $3.85\text{--}3.86\text{ \AA}^\circ$ (102), 3.03 \AA° (100), 2.84 \AA° (006), 2.49 \AA° (110), 2.28 \AA° (113), 2.09 \AA° (202), 1.97 \AA° (108), 1.87 \AA° (116) and 1.60 \AA° (212). Furthermore, the sample showed additional peaks prevailing at $3.33\text{--}3.34\text{ \AA}^\circ$ (101), 1.54 \AA° (211), 1.37 \AA° (203) and 1.28 \AA° (104) showed the presence of quartz [7]. Detailed clay mineralogy was investigated and identified by the characteristic reflections according to Moore and Reynolds [9].

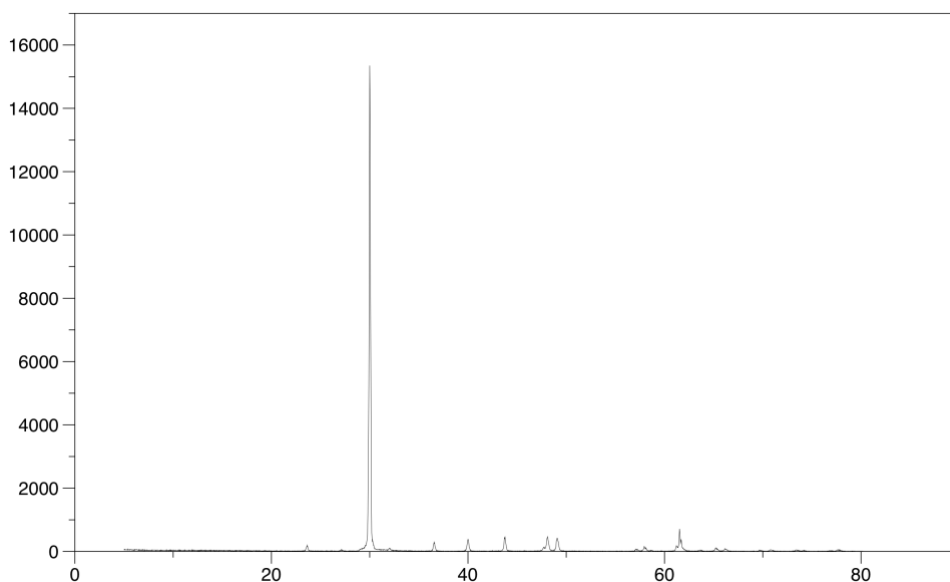


Fig. 2. X-RD of the limestone sample.

Fig. 3 shows the FTIR spectrum of the limestone sample. It shows the characteristic bands of calcite at $1,419$, 874.08 and 712.20 cm^{-1} . The spectrum peaks appearing at $1,799$ and $2,513.04\text{ cm}^{-1}$ are also an indication of the presence of calcite [10-13]. These data indicate that the studied limestone is mainly composed of calcium in the form of calcite as identified by its main absorption bands [13]. The reference bands observed at $1,419$, 874.08 and 712.20 cm^{-1} can be assigned to the asymmetric stretching, out-of-plane bending and in-plane bending modes of CO_3^{2-} , respectively [14]. Gunasekaran and Anbalagan mentioned in their research that the observed out-of-plane bending mode occurs at 877 cm^{-1} for ^{12}C .

This band shifts to lower wave numbers for other isotopes of carbon (^{13}C and ^{14}C). However, limestone sample has a splitting band at 874.71 cm^{-1} [12]. This clearly indicates that there is no isotopic shift. According to the author in his research, the bands observed at $1,799$ and $2,513\text{ cm}^{-1}$ are attributed to the $\nu_1 + \nu_4$ combination mode. Moreover, the stretching vibrations of the surface hydroxyl groups (Si-Si-OH or Al-Al-OH) were found at $3,544.52$ and $3,619.73\text{ cm}^{-1}$ [15]. Infrared techniques have been frequently used for the identification of clay minerals [10, 11] as well as the natural calcite minerals [12].

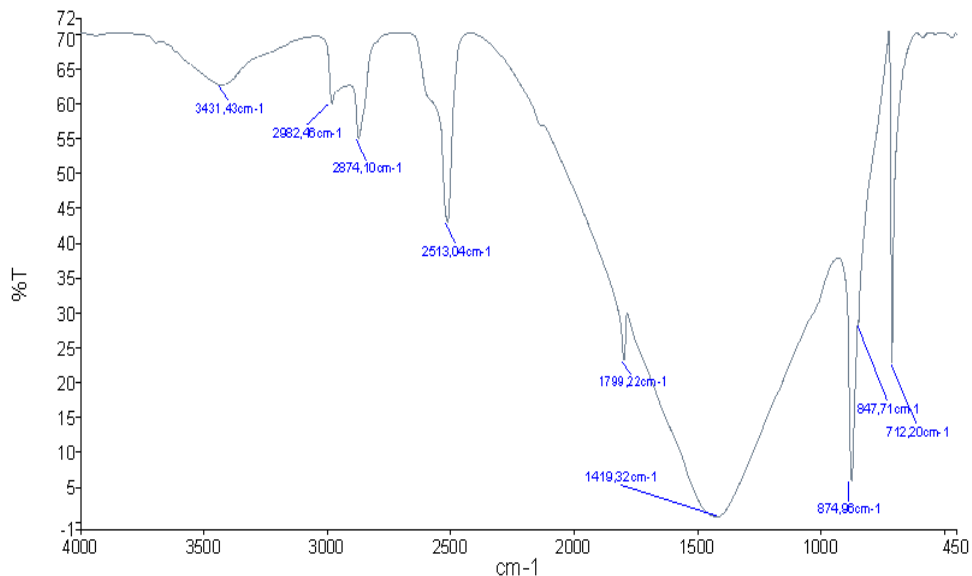


Fig. 3. FTIR spectrum of bulk limestone sample.

The observation of the morphology using the scanning electron microscope of the limestone, with three different sizes (fine, med, and coarse size) is reported in Fig. 4 a, b, and c respectively. It's clearly observed that the samples have different sizes due to different grinding and sieving processing applied on the samples. The samples show compact morphology, so the samples have less porous and the carbonates represent the main phase with calcite peaks [16]. Furthermore, the samples have morphology with angular grains of quartz size, covered with fine particles and the grains of calcite appear clearly. This analysis of the morphology by SEM is associated by EDS analysis of the elements exist on choised line on area with maximum amount of informations as it is showing in Fig. 4 and Table 2 respectively. The presence of Ca, O, and C, as major element confirms the importance of carbonate phases, CaCO_3 compound in the samples (Table 2).

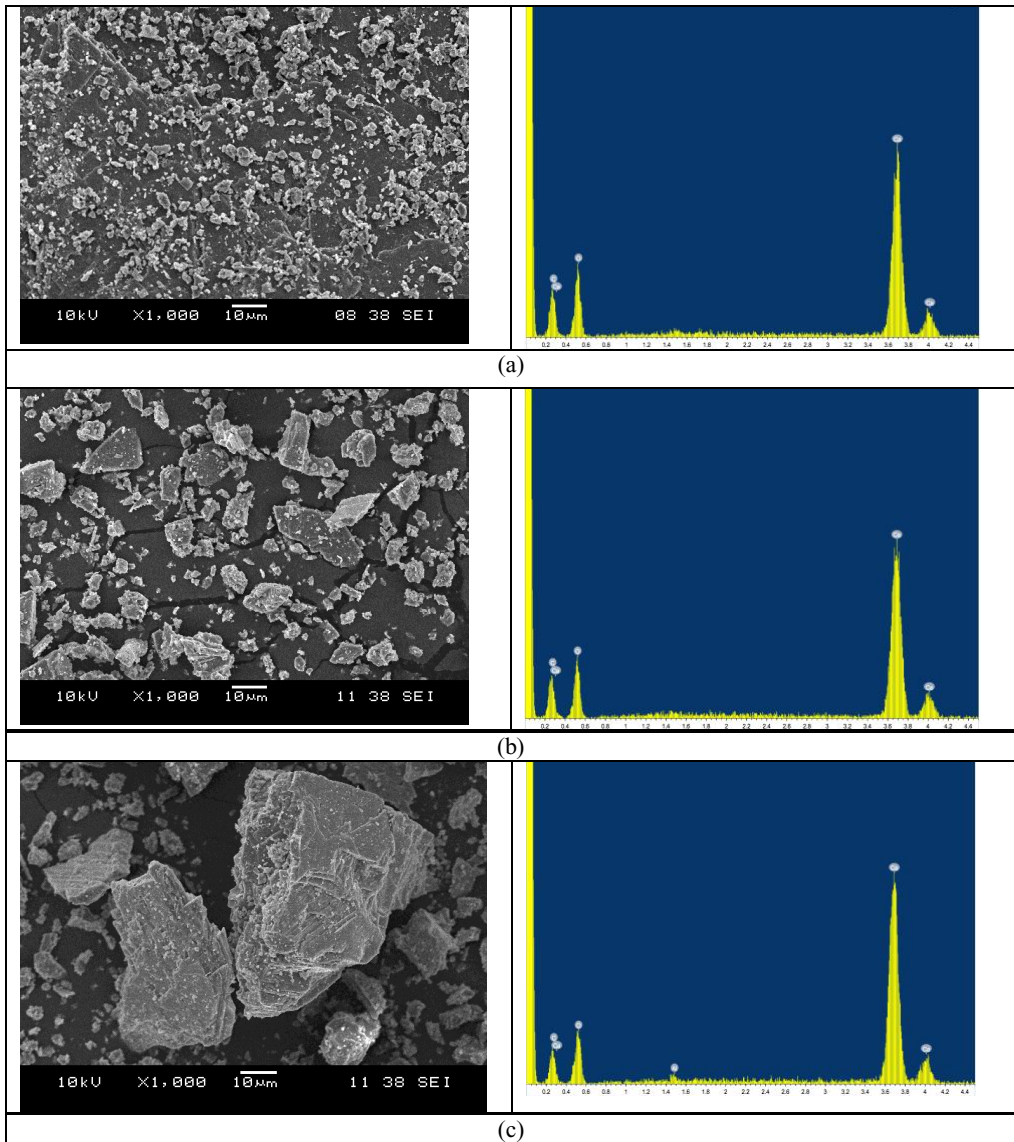


Fig. 4. SEM-EDS of lime stone samples at (a) fine size 75 µm (b) medium size 225 µm and (c) coarse size 425 µm.

Table 2. Elemental analysis of limestone samples.

Element	Weight%	Atomic %
C K	17.33	27.63
O K	45.69	54.70
Ca K	36.98	17.67
Total = 100		

4 Conclusions

In this work, it can be concluded that the limestone samples obtained from Bukit Keteri area had high limestone purity due to high calcium oxide and low silica percentage in the samples. Calcite mineral was identified by X-ray diffractograms and FTIR spectrum. Furthermore, the Ca, O, C elements proved the presence of CaCO₃ in the samples (as shown in SEM-EDS micrographs).

References

1. B. K. Tan, Bull. Eng. Geol. Environ. **35**, 57 (1987)
2. S. Cornelius, Jr. Hurlbut, K. Cornelis, *Dana's Manual of Mineralogy*, Wiley: New York, (1977)
3. M.E. Tucker, *Sedimentary Petrology: An Introduction to the Origin of Sedimentary Rocks*, Blackwell Scientific Publishing: Malden, (2001)
4. H.A. Aziz, M.N. Adlan, K.S. Ariffin, Bioresour. Technol. **99**, 1578 (2008)
5. R.J. Fairweather, M.A. Barlaz, J. Environ. Eng. **124**, 353 (1998)
6. R. Anderson, J.R. Jambeck, G.P. McCarron, Environmental Research and Education Foundation (2010)
7. A. Sdiri, T. Higashi, T. Hatta, F. Jamoussi, N. Tase, Environmental Earth Sciences **61**, 1275 (2010)
8. M. Felhi, A. Tlili, M.E. Gaied, M. Montacer, Appl Clay Sci **39**, 208 (2008)
9. D.M. Moore, R.C. Reynolds, *Quantitative analysis. In: Moore DM, Reynolds RC Jr (eds) X-Ray diffraction and the identification and analysis of clay minerals*, Oxford Univ Press: Oxford, 272, (1989)
10. Y.S. Al-Degs, M.I. El-Barghouthi, A.A. Issa, M.A. Khraisheh, G.M. Walker, Water Res **40**, 2645 (2006)
11. S.N. Preeti, B.K. Singh, Bull Mater Sci **30**, 235 (2007)
12. S. Gunasekaran, G. Anbalagan, Spectrochim. Acta, Part A **68**, 656 (2007)
13. S. Gunasekaran, G. Anbalagan, S. Pandi, J Raman Spectrosc **37**, 892 (2006)
14. N.V. Vagenas, A. Gatsouli, C.G. Kontoyannis, Talanta **59**, 831 (2003)
15. M. Hajjaji, S. Kacim, A. Alami, A. El Bouadili, M. El Mountassir, Appl Clay Sci **20**, 1 (2001)
16. K. Besnard, D.E.A. Hydrologie, G. Hydrogéologie, G.F. Hydrologie, Hydrogéologie, Géostatistique et Géochimie, Université Paris-Sud. (2000)